The Journal of Experimental Biology 204, 2423–2430 (2001)
Printed in Great Britain © The Company of Biologists Limited 2001
JEB3292

SPATIAL INTEGRATION IN POLARIZATION-SENSITIVE INTERNEURONES OF CRICKETS: A SURVEY OF EVIDENCE, MECHANISMS AND BENEFITS

THOMAS LABHART*, JÜRGEN PETZOLD AND HANSRUEDI HELBLING
Zoologisches Institut der Universität, Winterthurerstrasse 190, CH-8057 Zürich, Switzerland
*Author for correspondence (e-mail: labhart@zool.unizh.ch)

Accepted 19 April 2001

Summary

Many insects exploit the polarization pattern of the sky for compass orientation in navigation or cruising-course control. Polarization-sensitive neurones (POL1-neurones) in the polarization vision pathway of the cricket visual system have wide visual fields of approximately 60° diameter, i.e. these neurones integrate information over a large area of the sky. This results from two different mechanisms. (i) Optical integration; polarization vision is mediated by a group of specialized ommatidia at the dorsal rim of the eye. These ommatidia lack screening pigment, contain a wide rhabdom and have poor lens optics. As a result, the angular sensitivity of the polarization-sensitive photoreceptors is very wide (median approximately 20°). (ii) Neural integration; each POL1-neurone receives input from a large number of dorsal rim photoreceptors with diverging optical axes. Spatial integration in POL1-neurones acts as a spatial low-pass filter. It improves the quality of the celestial polarization signal by filtering out cloud-induced local disturbances in the polarization pattern and increases sensitivity.

Key words: polarization vision, photoreceptor, interneurone, model neurone, spatial integration, review, cricket, *Gryllus campestris*.

Introduction

Skylight polarization offers insects a useful reference in visual compass orientation for navigation or cruising-course control. The analysis of polarized skylight has been studied in a wide variety of arthropods (for reviews see Waterman, 1981; Wehner, 1997; Labhart and Meyer, 1999). The field cricket *Gryllus campestris* is one of the organisms in which knowledge about the neural mechanisms subserving polarization vision is most advanced. As in other insects (for a review, see Labhart and Meyer, 1999), polarization vision in crickets is mediated by a comparatively small group of specialized ommatidia situated at the dorsal rim of the compound eye (Burghause, 1979; Brunner and Labhart, 1987; Herzmann and Labhart, 1989). The photoreceptors of the dorsal rim area contain a blue-absorbing visual pigment (wavelength of maximal absorption, $\lambda_{max}\approx440$ nm) and are strongly sensitive to the oscillation plane (e-vector orientation) of plane-polarized light (polarization sensitivity PS≈10) (Labhart et al., 1984; Zufall et al., 1989; Blum and Labhart, 2000).

The e-vector information collected by the dorsal rim photoreceptors is processed by polarization-sensitive neurones in the optic lobe of the cricket, termed POL-neurones. In these neurones, spike activity is a sinusoidal function of e-vector orientation with alternating parts of excitation and inhibition, and with the maxima and the minima separated by 90° (Labhart, 1988). Thus, POL-neurones are polarization-opponent neurones receiving antagonistic input from two analyzer channels with orthogonal orientations of maximal sensitivity. The two analyzer channels are represented by the two sets of photoreceptors with orthogonally arranged microvilli that are present in each dorsal rim ommatidium (see Fig. 2C, lower right) (Burghause, 1979; Labhart, 1988). The polarization-antagonism makes the e-vector response of POL-neurones intensity-independent and enhances sensitivity for e-vector contrasts (Labhart, 1988). Of several morphological classes of POL-neurones found in the cricket's visual system, the POL1 class was best acccessible to electrophysiological experimentation (Petzold, 2001). There are three types of POL1-neurone that are tuned to different e-vector orientations (Labhart, 1988; Labhart and Petzold, 1993; Petzold, 2001); they may represent the input stage of a 'simultaneous' system of polarization vision, in which e-vector orientation is coded by the responses of three independent and differently tuned polarization-sensitive sensory channels (Bernard and Wehner, 1977; Lambrinos et al., 1997).

Another characteristic property of the POL1-neurones is the extent of their visual field. The visual field is remarkably wide, covering a large part of the upper sky, which indicates that POL1-neurones integrate e-vector information over a large area of the celestial polarization pattern (Labhart and Petzold, 1993; Petzold, 2001). What is the physiological basis of spatial integration in POL1-neurones? What is its functional significance? We will answer these questions in a brief survey of previous and new findings dealing with spatial integration in cricket POL1-neurones.

Visual field and e-vector tuning in POL1-neurones

In this paper, we present data on the best-studied morphological class of POL-neurone (designated POL1 by Petzold, 2001). These neurones receive dendritic input in the dorsalmost part of the medulla, have their cell body in the proximal part of the medulla and send a long axon through the brain to the contralateral optic lobe (see Fig. 5 in Labhart and Petzold, 1993; Petzold, 2001). Spike activity was recorded contralaterally, i.e. in the right optic lobe, from neurones receiving input from the cricket's left eye. The neurones were stimulated by small-field stimuli of plane-polarized blue light (≈2 ° diameter, 443 nm) at different positions of the visual field, and with the e-vector orientation rotating continuously forwards and backwards by 360 °. On the basis of the resulting modulation of spike frequency (for an example, see Fig. 3A), both the e-vector orientation of maximal spike frequency (Φ_{max}) and the amplitude of the e-vector response could be assessed (for technical details see Petzold, 2001).

There are three types of POL1-neurone that are tuned to different e-vector orientations. Presenting stimuli in the zenith (with respect to the natural head position), we found a trimodal distribution of Φ_{max} orientations consisting of three clearly separated peaks, indicating three types of POL1-neurone tuned to e-vectors approximately 10 °, 60 ° and 130 ° relative to the long axis of the head (see Fig. 1A for a circular histogram of the Φ_{max} values obtained in 142 POL1-neurones).

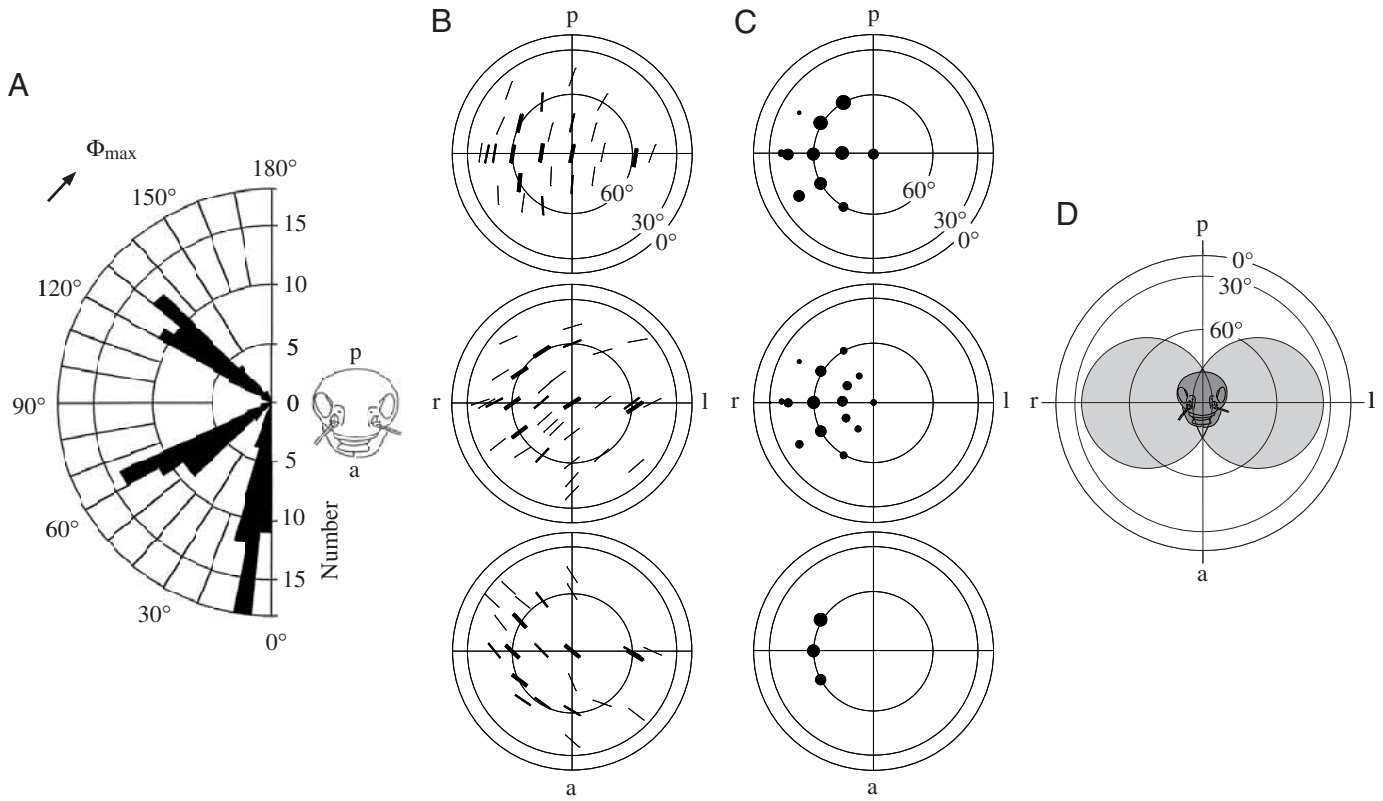

Fig. 1. e-vector tuning and visual field properties of POL1-neurones. (A) e-vectors eliciting maximal spike frequency (Φ_{max}) in 142 POL1-neurones stimulated with a zenithal stimulus. In this circular histogram, Φ_{max} is given with respect to the long axis of the head (the straight line connecting 0 ° and 180 °). The radial scale indicates the number of POL1-neurones found for any particular Φ_{max}. Note that there are three types of POL1-neurone tuned to approximately 10 °, 60 ° and 130 °. (B–D) Data are mapped on zenith projections of the upper visual hemisphere, i.e. the centre of each graph gives the zenith and the concentric circles represent parallels of latitude. (B) Φ_{max} orientation as a function of stimulus position in the three tuning types of POL1-neurone (upper, middle and lower graphs). The orientation of the bars indicates mean Φ_{max} values at their respective positions on the upper visual hemisphere. The width of the bars shows the number of measurements: thin, N=1; medium, N=2–5; thick, N>5. The numbers of POL1-neurones represented by each graph are 50, 48 and 44 (top to bottom). The Φ_{max} values are plotted with respect to the tangent to the parallel of latitude at the indicated positions (compare Fig. 2a in Schwind and Horváth, 1993). Thus, Φ_{max} can be read directly from the graphs; specifically, Φ_{max} orientations that are parallel within the visual field appear also parallel in the graph. Note that, for each e-vector type of POL1-neurone, Φ_{max} is quite independent of stimulus position. (C) Sensitivity as a function of stimulus position in the three tuning types of POL1-neurone. The diameter of the filled circles indicates mean relative sensitivity at their respective positions on the upper visual hemisphere (reference sensitivity of 1.0 at position 60 °/right). Numbers of measurements at each position range from 1 to 9 (for details, see Petzold, 2001). The numbers of POL1-neurones represented by each graph are 5, 8 and 9 (top to bottom). Data in A-C are from POL1-neurones in the left optic lobe receiving input from the cricket's left eye. (D) Position and size of the visual fields of POL1-neurones. The visual fields (approximate range of ≥25 % sensitivity; see text) are indicated by the grey areas for the POL1-neurones of both the right and the left optic lobe. r, right; l, left; a, anterior; p, posterior. Compiled from data in Petzold, 2001.

Using other stimulus positions, we found that all three e-vector types of POL1-neurone responded to polarized stimuli over much of the upper visual hemisphere. In Fig. 1B, the bars indicate the mean Φ_{max} orientations obtained for different stimulus positions mapped on a zenithal projection of the visual hemisphere, the width of the bars indicating the number of measurements (thin, N=1; medium, N=2–5; thick, N>5). By virtue of the mapping method chosen (see legend of Fig. 1), the Φ_{max} values can be read directly from the graphs; specifically, Φ_{max} orientations that are parallel in the visual field appear also parallel in the graphs. The data indicate clearly that e-vector tuning is independent of stimulus position, i.e. that Φ_{max} remains constant within the visual field of POL1-neurones.

Although the modulation amplitudes of the e-vector responses were similar for different stimulus positions, the contribution to the response from different parts of the visual field may differ when a POL1-neurone is exposed to the large-field stimulus of the sky. This is because of the characteristic intensity-independence of the e-vector response (Labhart, 1988; Petzold, 2001), which may mask sensitivity differences within the visual field when small-field stimuli are used. Thus, to determine a sensitivity profile for the visual field, the intensity-independence must be eliminated. This can be achieved by using stimuli of very low light intensity: below a certain quantum flux rate, the e-vector response of a POL1-neurone breaks down within approximately 1.5 log units of intensity (for an example, see Fig. 3A, bottom trace; Labhart, 1988; Petzold, 2001). At this low light level, a sensitivity profile can be determined in the usual way: the strength of the e-vector response for different positions is measured at one intensity, and relative sensitivity is calculated by comparing these responses to a response/intensity function as a calibrating curve (Petzold, 2001). Working near the absolute response threshold is difficult since small sensitivity fluctuations during the experiment are unavoidable, and for this reason the data proved to be quite noisy. Nevertheless, as indicated both by the data given in Fig. 1C (the diameter of the filled circles denotes relative sensitivity) and by evidence not presented here (Petzold, 2001), POL1-neurones have a relatively broad area of high sensitivity contralateral to the stimulated eye at approximately 60 ° elevation. From there, sensitivity decreases towards the margin of the visual field; for instance, sensitivity in the zenith is approximately 20–30 % compared with that in the centre of the visual field.

Our data show that the visual field of POL1-neurones is large. What size should be considered relevant under natural conditions? After taking into account all available data (Petzold, 2001), we adopted a visual field diameter of 60 °, which is particularly pertinent for simulation experiments (see below). This area corresponds roughly to that part of the visual field that is defined by at least 25 % sensitivity. This rather conservative estimate disregards the outer, low-sensitivity range of the visual field. However, computer simulations show that an increase of the visual field to 90 ° has little influence on the response of a POL1-neurone to the polarization pattern (Petzold, 2000; J. Petzold, unpublished data). The available data indicate that the visual fields of the three e-vector types of POL1-neurone overlap extensively, and we assume them to be identical; this view is in accordance with the data presented below. In the summarizing graph of Fig. 1D, the grey areas depict the visual fields assumed for all POL1-neurones of both the right and the left sides.

Optical integration by photoreceptors

The ommatidia of the dorsal rim area (DRA) are anatomically and optically specialized. This is obvious even in the intact cricket eye: the DRA has a pale, whitish appearance and the surface of the cornea is flat, unlike the adjacent dorsal area, which is brown and has normal convex corneal facets. Histological sections of the retina revealed that screening pigment is either completely lacking or strongly reduced in the DRA (Fig. 2A) (Burghause, 1979; Brunner and Labhart, 1987). In addition, the rhabdoms are much wider in the DRA than in the rest of the eye (Fig. 2A). The corneal lenses of the DRA have only half the normal diameter. The optical quality of the lenses in the dorsalmost rows of ommatidia is poor. The lenses of the other DRA ommatidia are of good optical quality but, compared with the lenses of normal ommatidia, both inner and outer lens curvatures are altered in such a way that the focal length is decreased, i.e. the ommatidia are under-focused (Ukhanov et al., 1996).

All these specializations (no screening pigment, wide rhabdoms, small lenses and non-focusing or under-focusing) degrade the optical quality of the ommatidia in the DRA. As demonstrated by electrophysiological recordings, this has severe consequences for the acceptance angle of the photoreceptors: compared with the normal ommatidia, the visual fields are greatly enlarged in the DRA. Whereas the acceptance angle $\Delta\rho$ is approximately 6 ° in the unspecialized dorsal part of the eye, the median value of $\Delta\rho$ is approximately 20 ° in the DRA. In addition, visual field size varies strongly in the DRA, ranging from 6 ° to 67 ° (Labhart et al., 1984; Blum and Labhart, 2000). This variation is due to pronounced variations in the screening pigment content of the ommatidia (Burghause, 1979; Brunner and Labhart, 1987) and in the optical quality and focal distance of the corneal lenses (Ukhanov et al., 1996). Fig. 2B gives examples of visual fields measured in both the DRA (upper graphs) and the regular dorsal area (lower graphs).

Thus, the photoreceptors of the DRA integrate optically over quite a large area of the sky. Interestingly, the interommatidial angle $\Delta\varphi$ of approximately 1 ° is much smaller than the acceptance angle of typically 20 °. The divergence between the optical axes is so small that the ommatidia within a given section of the DRA receive light from practically the same area of the sky and, thus, spatial resolution is virtually abolished. This is illustrated in Fig. 2C, in which the visual fields of three neighbouring ommatidia are overlaid on a schematic representation of the DRA.

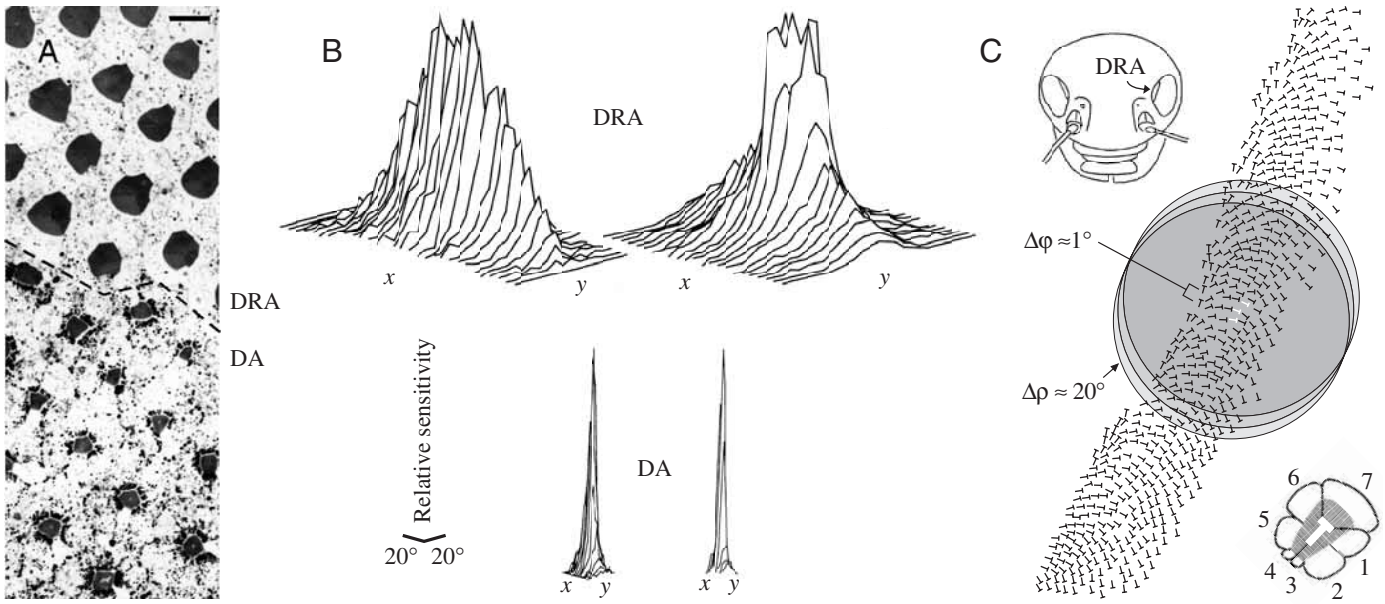

Fig. 2. Anatomical and optical properties of the dorsal rim area of the eye. (A) Light micrograph of a tangential section through the dorsalmost part of the eye. Note the missing screening pigment and the enlarged, trapezoidal rhabdoms in the ommatidia of the dorsal rim area (DRA, top). The much smaller rhabdoms of the unspecialized dorsal ommatidia (DA, bottom) are densely surrounded by screening pigment. Scale bar, 10 μm. (B) Three-dimensional representations of photoreceptor visual fields in the DRA (above) and in the unspecialized DA of the eye (below). The *x* and *y* directions are parallel and perpendicular, respectively, to the elongated DRA. (C) Comparison between visual field size and interommatidial angle of photoreceptors in the DRA. The T symbols indicate position and orientation of the retinulae within the dorsal rim area (compare enlarged cross-section through an ommatidum at the lower right; cells are numbered according to Burghause, 1979). Typically sized visual fields (in grey; acceptance angle $\Delta\rho \approx 20°$) of three adjacent ommatidia (in white) are overlaid on a schematic representation of a cross-section through part of the dorsal rim area. The angular distance between the rhabdoms (interommatidial angle $\Delta\varphi$) is approximately 1 °. Note that the visual fields overlap extensively. (A) After Labhart and Petzold, 1993; (B) after Labhart et al., 1984; (C) according to data by Blum and Labhart, 2000.

Neural integration by POL1-neurones

What is the topological relationship between the ommatidia of the DRA and the POL1-neurones? Does each POL1-neurone receive input from just one ommatidium or from a large number of ommatidia? Do the three e-vector types of POL1-neurone correlate with different parts of the DRA or do they receive input from ommatidia in the whole DRA? To answer these questions, we undertook two series of electrophysiological experiments.

In the first series, we compared the responses of the POL1-neurones with those of the polarization-sensitive dorsal rim photoreceptors at very low light intensities, typical examples of which are shown in Fig. 3. The dark-adapted cells were stimulated with polarized blue light in the centre of their visual field, and the e-vector orientation was rotated forwards and backwards by 360 ° (see ascending and descending line at the bottom of Fig. 3A,B). In POL1-neurones, the spike frequency modulation elicited by the rotating e-vector is intensity-independent, but at very low intensities the response breaks down (see above; Labhart, 1988; Petzold, 2001). The signal trace at the bottom of Fig. 3A indicates the threshold response of a POL1-neurone, i.e. at a light intensity that elicits half the normal frequency modulation. At this light intensity, the strongly polarization-sensitive photoreceptor (PS≈10) absorbs approximately 1 photon s^{-1} in a quite random fashion and no response modulation can be detected (see quantum bumps in bottom trace of Fig. 3B). At a light intensity approximately 1 log unit higher, the POL1-neurone response is already maximal while the receptor response still shows no clear modulation (compare second traces from bottom in Fig. 3A,B). It takes roughly 10^3 times the threshold intensity of the POL1-neurone for the photoreceptor to produce a reliable response (see top trace in Fig. 3B). Our qualitative comparison between the POL1-neurone and receptor responses clearly shows that the POL1-neurones receive input from a large number of photoreceptors or ommatidia.

In the second set of experiments, we measured the responses of POL1-neurones to selective stimulation of different parts of the DRA: a typical example is shown in Fig. 4A. The dorsal part of the eye was illuminated with a slit of blue light stimulating a frontal, middle or posterior section of the DRA (see Fig. 4A, left) and the e-vector orientation was rotated forwards and backwards by 360 °. As exemplified in Fig. 4A, right, the POL1-neurones responded to all three modes of stimulation. In addition, the maximal activity was at almost the same e-vector orientation for the different slit positions (see vertical grey lines connecting the three response traces in Fig. 4A). This was found for all three e-vector types of POL1-neurone: in the 11 neurones tested (five of the 10 ° type, four of the 60 ° type and two of the 130 ° type), the Φ_{max} values

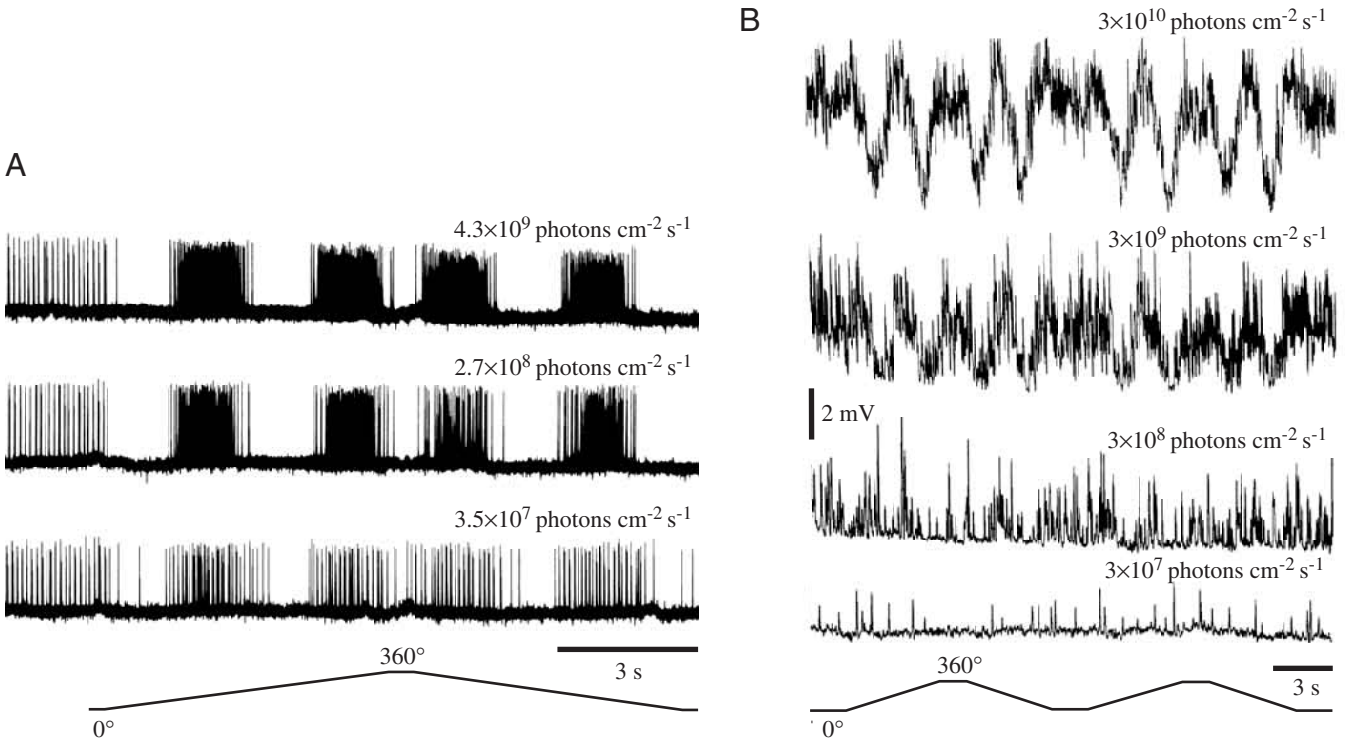

Fig. 3. Responses of a POL1-neurone (A) and a polarization-sensitive photoreceptor (PS≈10) of the dorsal rim area (B) to rotating e-vector orientation at very low light intensities. The dark-adapted cells were stimulated with a small-field blue stimulus (2° diameter, 443 nm for A, 1° diameter, 440 nm for B) positioned in the centre of their visual fields, and the e-vector orientation was rotated forwards and backwards by 360° (see ascending and descending line at the bottom of the graphs). Light intensity is indicated at the upper right of each response trace. Light intensity increases in steps of approximately 1 log unit from the bottom to the top traces. The bottom trace in A shows the threshold response of the POL1-neurone (half-maximal response). Note that the photoreceptor absorbs only approximately 1 photon s^{-1} in a random fashion at the same light intensity (see quantum bumps in bottom trace of B), i.e. no response modulation can be detected. (A) The first 2 s of the POL1-neurone traces show spontaneous activity in the dark. (For details of the electrophysiological recording technique, see Blum and Labhart, 2000; Petzold, 2001.)

obtained for the three slit positions generally differed by less than 10°; the maximal difference was only 10.6°. As illustrated in Fig. 4B, these experiments demonstrate that each e-vector type of POL1-neurone (represented by the coloured, double-arrowed circles) receives input from the anterior, middle and posterior sections of the DRA, i.e. probably from the whole DRA. As indicated by the differently oriented T symbols in Fig. 4B, the orientations of the dorsal rim ommatidia exhibit the pattern of a distorted fan such that each section of the DRA contains differently oriented ommatidia in a semicircular arrangement. We conclude that each tuning type of POL1-neurone collects input from ommatidia of appropriate orientation (exemplified by the coloured T symbols). Since only relatively few ommatidia are optimally oriented for each tuning type, we believe that ommatidia with intermediate orientations (up to ±20–30° deviation from the optimum) also contribute to the POL1-neurone input. Including these incompletely aligned ommatidia reduces the overall polarization sensitivity of the system to some degree, but increases absolute sensitivity and, thus, signal-to-noise ratio (see below). Model calculations based on the ommatidial arrangement in the DRA of the ant *Cataglyphis bicolor* indicate that ommatidial misalignment of a degree expected for the input ommatidia of cricket POL1-neurones has only a moderate effect on the modulation amplitude of the neurone response. Thus, using a field of parallel e-vectors for stimulus (as present in the strongly polarized band of the sky crossing the zenith at low solar elevations) and rotating the model under this sky, the modulation amplitude decreased by only approximately 15 % as a result of misaligment (Petzold, 2001).

Functional significance of spatial integration

Spatial integration means that spatial resolution must be abandoned within the integration area. Apparently, the POL1-neurones are insensitive to the fine structure of skylight polarization but respond to the overall polarization signal within their large visual fields. What is the functional significance of spatial integration in POL1-neurones?

To study this question, we used an opto-electronic device that implemented the characteristic properties of cricket POL1-neurones, i.e. polarization opponency, position-independent e-vector tuning, blue sensitivity and a visual field of 60° diameter centred at 65° elevation (for details, see Labhart,

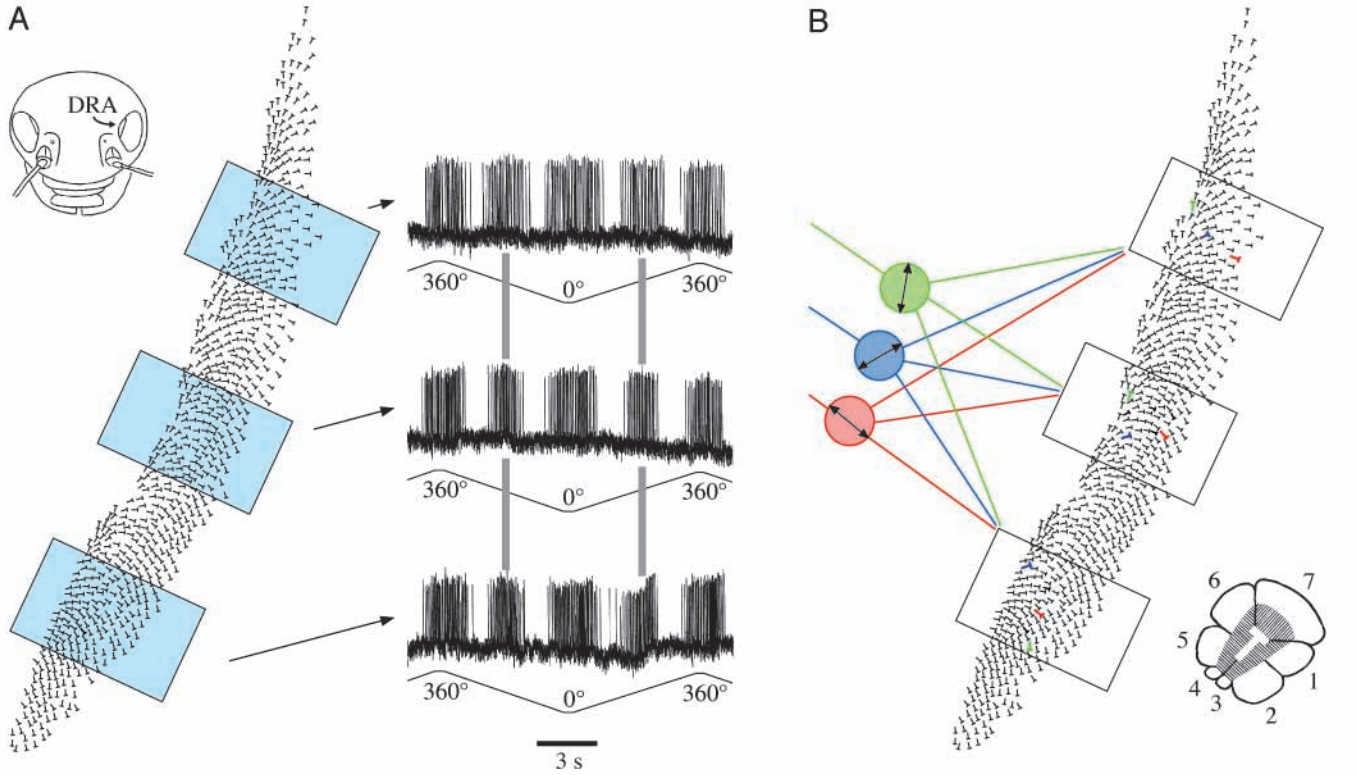

Fig. 4. (A) Response of a POL1-neurone to selective stimulation of different parts of the dorsal rim area (DRA). Left, stimulus situation; right, response traces. The dorsal part of the eye was illuminated with a slit of blue light (≈150 µm wide, 443 nm) stimulating a frontal, middle or posterior section of the dorsal rim area (which is represented schematically as in Fig. 2C), and the e-vector orientation was rotated forwards and backwards by 360 ° (see ascending and descending line below the response traces). Note that the POL1-neurone responds to all three modes of stimulation, showing maximal activity at the same e-vector orientation (see vertical grey lines connecting the response traces). (For details of the electrophysiological recording technique, see Petzold, 2001.) (B) Neural integration in POL1-neurones. Interpretation of both the selective stimulation experiments as exemplified in A and the threshold stimulation experiments shown in Fig. 3. (i) All three e-vector types of POL1-neurone (represented by the coloured, double-arrowed circles) receive input from a large number of ommatidia along the whole dorsal rim area. (ii) Each e-vector type receives input from ommatidia of appropriate orientation, as exemplified by the coloured T symbols in each box (compare enlarged cross-section through an ommatidum at the lower right).

1999). The instrument was tuned to horizontal e-vector orientations. Although none of the real POL1-neurones is maximally sensitive to this e-vector orientation, horizontal tuning is optimal for assessing the strength and the reliability of the polarization signal in the sky (see Labhart, 1999). Combining the properties of a technical measuring instrument with those of a real insect neurone, our neuromimetic, field-proof device allowed us to study sky-light polarization in an insect-relevant way by providing a cricket's eye view of the polarization pattern.

To measure the activity of the model POL1-neurone for different azimuth orientations with respect to the polarization pattern, the instrument scanned the sky by making a 360 ° turn around its vertical axis. The resulting signal simulates the modulation of POL1-neurone activity as a cricket makes a 360 ° turn under the sky. We collected data for a wide range of sky conditions (cloudless, cloudy, overcast) and solar elevations (0 ° to 44 °) (Labhart, 1999).

Under cloudless skies, the activity was always maximal when the instrument was directed exactly to either the solar or the antisolar azimuth. This was to be expected since, at these directions, the e-vector tuning orientation (horizontal) of the instrument matches the horizontal e-vector orientation in the sky [see bars along the symmetry line (vertical line) of the polarization patterns in Fig. 5A].

Under cloudy skies, the activity maxima still indicated the solar and the antisolar azimuth with surprising precision, as illustrated by three examples: for an evenly cloud-scattered sky, for a sky with a large, asymmetrical cloud, and for a widely overcast sky (Fig. 5B–D, respectively). For those skies in which the effective degree of polarization (as indicated by the modulation amplitude of the signal; see Labhart, 1999) was above the detection threshold of cricket POL1-neurones of 5 % (thus, excluding strongly overcast skies), the maxima deviated by only ±2.3 ° and ±3.4 ° (s.d.) from the solar or the antisolar azimuth, respectively, and the largest error was just 12 ° (Labhart, 1996; Labhart, 1999). To test the influence of the size of the visual field on the performance of the model neurone, we also took measurements with strongly reduced apertures (Labhart,

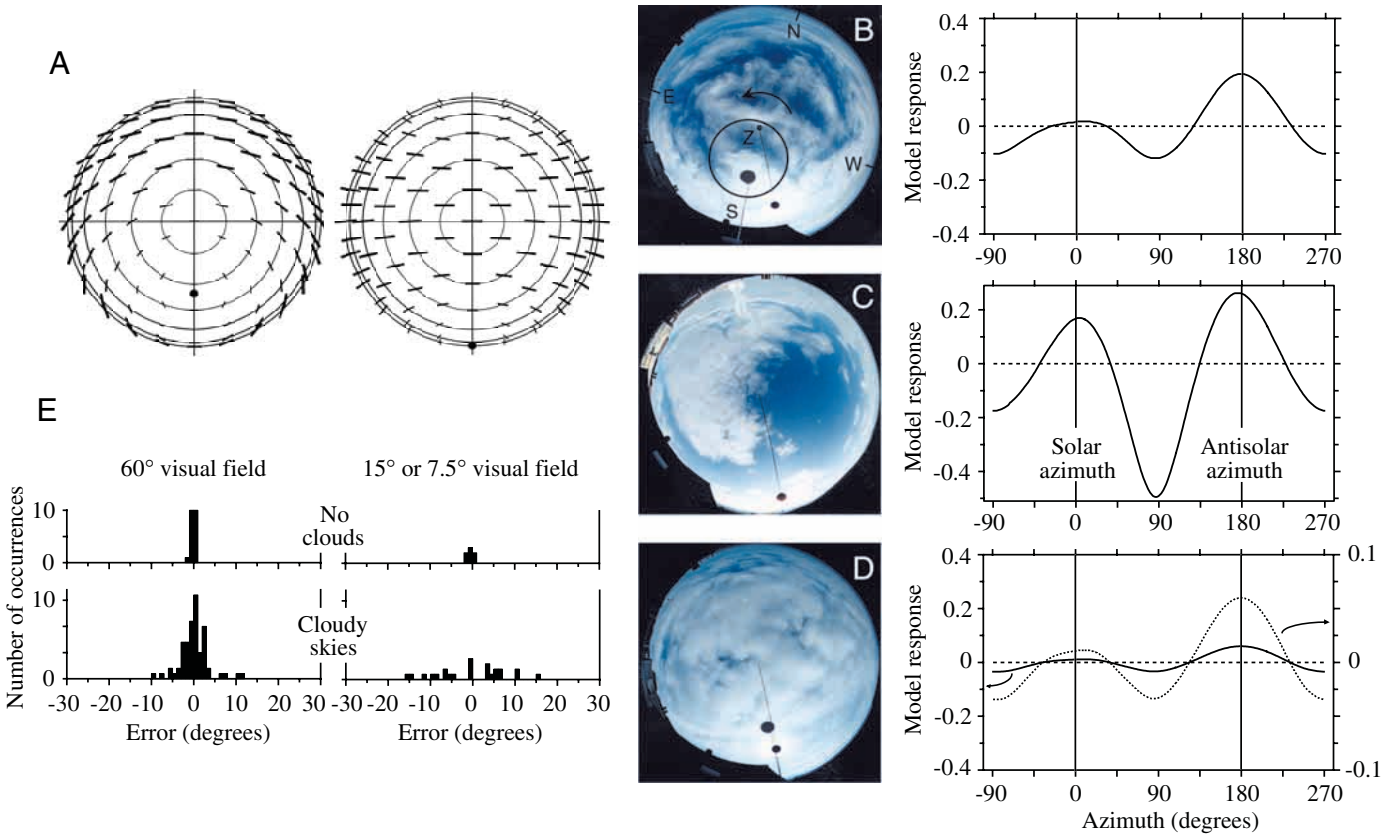

Fig. 5. (A) Polarization pattern of the sky for two elevations of the sun (filled circle; left, 55 °; right, 5 °). In this two-dimensional representation of the polarization pattern, the concentric circles indicate parallels of latitude of the celestial hemisphere with the zenith at the centre. e-vector orientations (indicated by the bars) are plotted with respect to the tangent to the parallel of latitude at the indicated positions (compare Fig. 2a in Schwind and Horváth, 1993). In this representation of the polarization pattern, e-vector orientations can be read directly from the graph; specifically, e-vectors that appear parallel in the sky also appear parallel in the graph. The degree of polarization is indicated by the length and width of the bars. Note that e-vector orientation in this figure is mapped the same way as Φ_{max} in Fig. 1B. (B–D) Responses of an opto-electronic model POL1-neurone to natural skylight polarization. Three examples for different cloud conditions are shown. Left, 180 ° fisheye photographs indicating actual sky conditions; (B) a loosely cloud-scattered sky, (C) an asymmetrically clouded sky and (D) a heavily clouded sky. The zenith is at the centre (see Z in B), and the horizon is at the circumference of the photographs. The black disks in the photograph are sun screens that shade the photograph and the model neurone from direct sun light. The small disk indicates the position of the sun, and the thin line extending from below the disk gives the symmetry line of the polarization pattern (compare with A). The circle in B indicates the outline of the 60 ° visual field of the model. The bright 8-shaped area near the antisolar horizon in C is caused by reflections of sunlight in the camera lens. Right, response curves of the model to the skies on the left obtained by scanning the sky through 360 °. Ordinate, response in dimensionless logarithmic units (solid line) (see Labhart, 1999); abscissa, orientation of the model with respect to the polarization pattern. Dotted line in D shows the response on a larger scale (right ordinate) Since the model is tuned to horizontal e-vector orientations, the response maxima are indicators of the solar (0 °) and the antisolar (180 °) azimuth (compare with A). The response curves show that, even under cloudy skies, the maxima deviate only little from the solar or antisolar azimuth. (E) Performance of the model POL1-neurone with a large (60 °) and a small (15 ° or 7.5 °) visual field. The histograms indicate the deviation (error) of the antisolar response maximum from the antisolar azimuth under clear (upper graphs) and cloudy (lower graphs) skies. The ordinate indicates the number of occurrences (measurements). Note the inferior directional performance (larger errors) with small visual fields (compare the left and right lower graphs). The effective degree of polarization was ≥10 % for this comparative study. (B-E were compiled from data in Labhart, 1999)

1999). Fig. 5E compares the performance of the model neurone with the standard large (60 °) and small (7.5 ° or 15 °) visual fields (left versus right histograms). For cloudless skies, the errors were very small and independent of visual field size (compare upper histograms). However, under cloudy skies, the errors were much larger with the small apertures (compare lower histograms). Apparently, spatial integration over a wide area of the sky improves the precision of the polarization signal under unfavourable sky conditions.

Our field experiments with the model POL-neurone show that spatial integration by the large visual field of cricket POL1-neurones acts as a spatial low-pass filter that serves to even out local disturbances in sky-light polarization. Since the e-vector tuning orientation is independent of stimulus position (see Fig. 1B), POL1-neurones respond to a weighted average of e-vector orientation in the upper part of the sky.

A second benefit of optical and neural integration is the gain in sensitivity. For the dorsal rim photoreceptors, the sensitivity

gain due to the increase in visual field size was estimated to be 5- to 20-fold for an extended light source such as the sky (Labhart et al., 1984). Compared with the large field sizes, this factor seems quite small, but one must consider that, in our case, the increase in visual field size is a result of degraded optics and is not the effect of a proper reduction in focal length (*f*-number reduction), which conserves the quality of the optics. The sensitivity of the POL1-neurones is further enhanced by integrating the signals of some 200 ommatidia (one-third of all dorsal rim ommatidia). The resulting increase in signal-to-noise ratio is particularly useful at low light levels and with low degrees of polarization. Field crickets respond to polarized light at intensities that are lower than under the clear, moonless night sky (Herzmann and Labhart, 1989). Because of both clouds and high solar elevation (see Fig. 5A, left), the effective degree of polarization in the sky is often quite low: the median of our sample obtained with the model POL-neurone was only 13 % for the solar and 28 % for the antisolar half of the sky, and the value never exceeded 53 % (Labhart, 1999). Thus, the low detection threshold of 5 % polarization (Labhart, 1996) is certainly justified, especially since even such weak polarization signals contain useful directional information (Labhart, 1999). Apart from low-pass filtering in the spatial domain, the photoreceptors of the DRA have temporal low-pass properties. Compared with the receptors in the unspecialized parts of the eye, their responses to both light flashes and sinusoidal modulation of light intensity are sluggish (Labhart et al., 1984; Zufall et al., 1989; T. Labhart, unpublished data), indicating a substantial increase in shutter time.

In addition to crickets, a number of other insect species from different orders also benefit from spatial integration in polarized skylight orientation. Clear evidence for optical integration has been found in members of the Orthoptera, Coleoptera and Hymenoptera. In some of them, the visual fields of the dorsal rim photoreceptors are increased by sacrificing optical isolation between the ommatidia (lack of pigment or tracheal screen) and/or by the unmatched focal length of the corneal lenses, i.e. in a similar way as in crickets. In addition, light-diffusing structures have been observed in the cornea of several species (for a review, see Labhart and Meyer, 1999). Although the visual fields of the dorsal rim ommatidia are not extended in desert ants *Cataglyphis* sp. (no optical integration), there is evidence for neural integration. Both electrophysiological recordings from *Cataglyphis* POL-neurones (Labhart, 2000) and behavioural experiments (Wehner, 2001) indicate that e-vector information from different parts of the sky is pooled.

This work was supported by the Swiss National Science Foundation grant 31-43317.95 (to R. Wehner, T. Labhart and E. Meyer). We thank Dr Rüdiger Wehner for critical comments on the manuscript.

References

Bernard, G. D. and Wehner, R. (1977). Functional similarities between polarization vision and color vision. *Vision Res.* **19**, 1017–1028.

Blum, M. and Labhart, T. (2000). Photoreceptor visual fields, ommatidial array, and receptor axon projections in the polarization-sensitive dorsal rim area of the cricket compound eye. *J. Comp. Physiol.* A **186**, 119–128.

Brunner, D. and Labhart, T. (1987). Behavioural evidence for polarization vision in crickets. *Physiol. Ent.* **12**, 1–10.

Burghause, F. M. H. R. (1979). Die strukturelle Spezialisierung des dorsalen Augenteils der Grillen (Orthoptera, Grylloidea). *Zool. Jb. Physiol.* **83**, 502–525.

Herzmann, D. and Labhart, T. (1989). Spectral sensitivity and absolute threshold of polarization vision in crickets: a behavioral study. *J. Comp. Physiol. A* **165**, 315–319.

Labhart, T. (1988). Polarization-opponent interneurons in the insect visual system. *Nature* **331**, 435–437.

Labhart, T. (1996). How polarization-sensitive interneurones of crickets perform at low degrees of polarization. *J. Exp. Biol.* **199**, 1467–1475.

Labhart, T. (1999). How polarization-sensitive interneurones of crickets see the polarization pattern of the sky: a field study with an opto-electronic model neurone. *J. Exp. Biol.* **202**, 757–770.

Labhart, T. (2000). Polarization-sensitive interneurons in the optic lobe of the desert ant *Cataglyphis bicolor*. *Naturwissenschaften* **87**, 133–136.

Labhart, T., Hodel, B. and Valenzuela, I. (1984). The physiology of the cricket's compound eye with particular reference to the anatomically specialized dorsal rim area. *J. Comp. Physiol. A* **155**, 289–296.

Labhart, T. and Meyer, E. P. (1999). Detectors for polarized skylight in insects: a survey of ommatidial specializations in the dorsal rim area of the compound eye. *Microsc. Res. Tech.* **47**, 368–379.

Labhart, T. and Petzold, J. (1993). Processing of polarized light information in the visual system of crickets. In *Sensory Systems of Arthropods* (ed. K. Wiese, F. G. Gribakin, A. V. Popov and G. Renninger), pp. 158–168. Basel, Boston, Berlin: Birkhäuser Verlag.

Lambrinos, D., Maris, M., Kobayashi, H., Labhart, T., Pfeifer, R. and Wehner, R. (1997). An autonomous agent navigating with a polarized light compass. *Adaptive Behav.* **6**, 131–161.

Petzold, J. (2001). Polarisationsempfindliche Neuronen im Sehsystem der Feldgrille, *Gryllus campestris*: Elektrophysiologie, Anatomie und Modellrechnungen. PhD thesis, University of Zürich.

Schwind, R. and Horváth, G. (1993). Reflection-polarization patterns at water surfaces and correction of a common representation of the polarization pattern of the sky. *Naturwissenschaften* **80**, 82–83.

Ukhanov, K. Y., Leertouwer, H. L., Gribakin, F. G., and Stavenga, D. G. (1996). Dioptrics of the facet lenses in the dorsal rim area of the cricket *Gryllus bimaculatus*. *J. Comp. Physiol. A* **179**, 545–552.

Waterman, T. H. (1981). Polarization sensitivity. In *Comparative Physiology and Evolution of Vision in Invertebrates* B, *Invertebrate Visual Centers and Behavior* I (ed. H. Autrum), pp. 281–469. Berlin, Heidelberg, New York: Springer Verlag.

Wehner, R. (1997). The ant's celestial compass system: spectral and polarization channels. In *Orientation and Communication in Arthropods* (ed. M. Lehrer), pp. 145–185. Basel: Birkhäuser Verlag.

Wehner, R. (2001). Polarization vision – a uniform sensory capacity? *J. Exp. Biol.* **204** 2589–2596.

Zufall, F., Schmitt, M. and Menzel, R. (1989). Spectral and polarized light sensitivity of photoreceptors in the compound eye of the cricket (*Gryllus bimaculatus*). *J. Comp. Physiol. A* **164**, 597–608.